Problem-Statement

Let an object have a reflectance given by r. Then the complex-distribution of the object-field is given by $g \sim CN(0, D(r))$ [1]. The problem statement is given

$$y = Ag + w$$

we would like to estimate r.

1 Case I: Linear measurements $(A = I)$

1.1 Forward-model:

Let the reflectance of the object that is imaged be given by $r \in [0, 1]$. Under the assumed model of the object-filed given by $g \sim CN(0, D(r))$, and the additive white-gaussian noise model we have that the measured complex-signal is given as

$$y = g + w.$$

A single-realization of this is given in Figure with std. deviations of the noise at $\sigma_w = \{0.001, 0.1\}$.

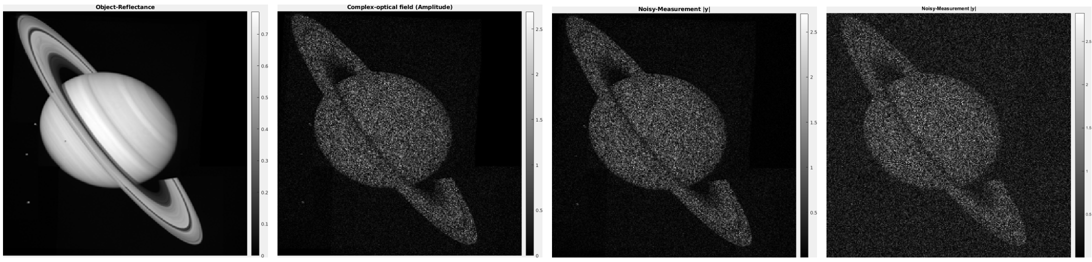

(a) Reflectance (r) (b) Optical-Field ($|g|$) (c) ($|y|$) $\sigma = 0.001$ (d) ($|y|$) $\sigma = 0.1$

Figure 1: An example-realization of the forward-model $y = g + w$. Two realizations of the noisy observations are shown at std. deviations of $\{0.001, 0.1\}$.

1.2 ML-estimate

The likelihood of the measurements y is given as $p(y|r) \sim CN(0, D(r) + \sigma_w^2 I)$. Applying the maximum-likelihood estimator to the above problem we have

$$\begin{aligned}
\hat{r} &= \arg\max \log p(y|r) \\
&= \arg\max \frac{-1}{2}\left(\log\left((2\pi)^N |D(r) + \sigma_w^2 I|\right) + y^H (D(r) + \sigma_w^2 I)^{-1} y \right) \\
&= \arg\max \frac{-1}{2}\left(\sum_{i=1}^{N} \log\left(2\pi(r_i + \sigma_w^2)\right) + \frac{|y_i|^2}{r_i + \sigma_w^2} \right) \\
\implies \hat{r_i} &= \arg\max \frac{-1}{2}\left(\log\left(2\pi(r_i + \sigma_w^2)\right) + \frac{|y_i|^2}{r_i + \sigma_w^2} \right) \\
&= \arg\min \log\left(2\pi(r_i + \sigma_w^2)\right) + \frac{|y_i|^2}{r_i + \sigma_w^2}.
\end{aligned}$$

Taking the differential of the above equation and equating to zero we get the ML estimate

$$\hat{r}_i \;=\; |y_i|^2 - \sigma_w^2.$$

The reconstructions for varying degrees of noise is shown in Figure 3 (a-d).

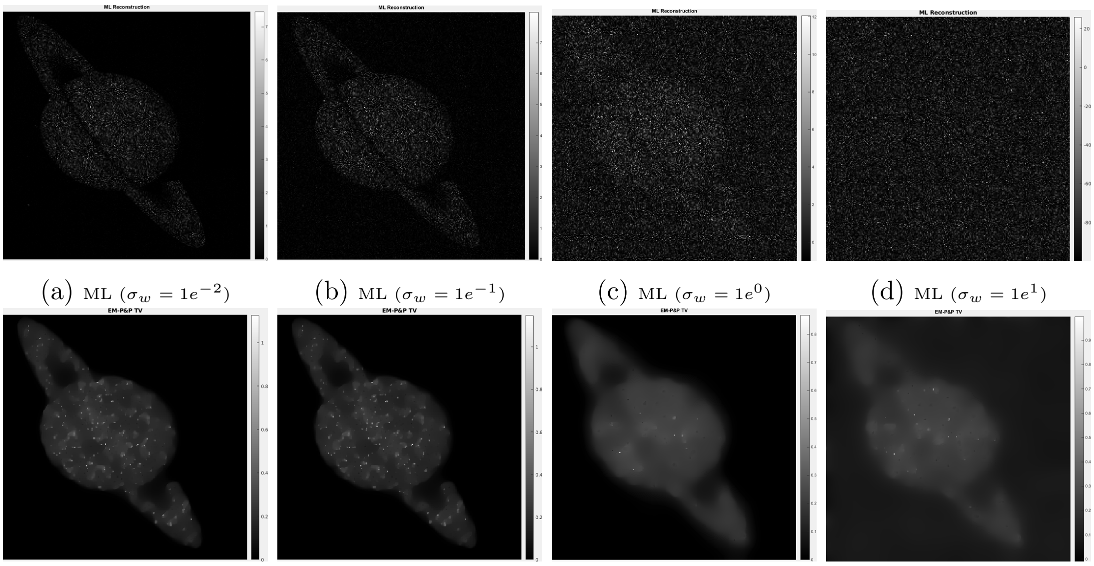

(a) ML ($\sigma_w = 1e^{-2}$) (b) ML ($\sigma_w = 1e^{-1}$) (c) ML ($\sigma_w = 1e^{0}$) (d) ML ($\sigma_w = 1e^{1}$)

(e) PnP-TV ($\sigma_w = 1e^{-4}$) (f) PnP-TV ($\sigma_w = 1e^{-3}$) (g) PnP-TV ($\sigma_w = 1e^{-2}$) (h) PnP-TV ($\sigma_w = 1e^{-1}$)

Figure 2: An example-realization for different inversion-models. The inversions are shown for different std. deviations of $\{1e^{-4}, 1e^{-3}, 1e^{-2}, 1e^{-1}\}$.

1.3 Plug and play (PnP) estimate (MAP)

The MAP estiamate for the above problem is given as

$$\begin{aligned}\hat{r} &= \arg\min -\log p(r|y) \\ &= \arg\min -\log p(y|r) - \log p(r). \end{aligned} \tag{1}$$

The PnP algorithm [2] decouples the above problem into one where we can apply the forward and prior models in the form of denoisers. Specifically, the PnP algorithm operates by splitting the unknown variable r into two variables r, v and converts the unconstrained optimization problem in (1) into a constrained optimization problem

$$\hat{r} = \underset{r=v}{\arg\min}\; \ell(r) + \beta s(v) \tag{2}$$

where $\beta s(v) = p(v)$ is the prior term and $\ell(r)$ enforces the meausrement constraints on r. Adopting an ADMM approach to solve the above problem results in an algorithm containing two primary operations:

(1) **Inversion operator**

$$F(\tilde{r}, \sigma_\lambda) = \arg\min_r \left\{ \ell(r) + \frac{1}{2\sigma_\lambda^2}\|r - \tilde{r}\|^2 \right\},$$

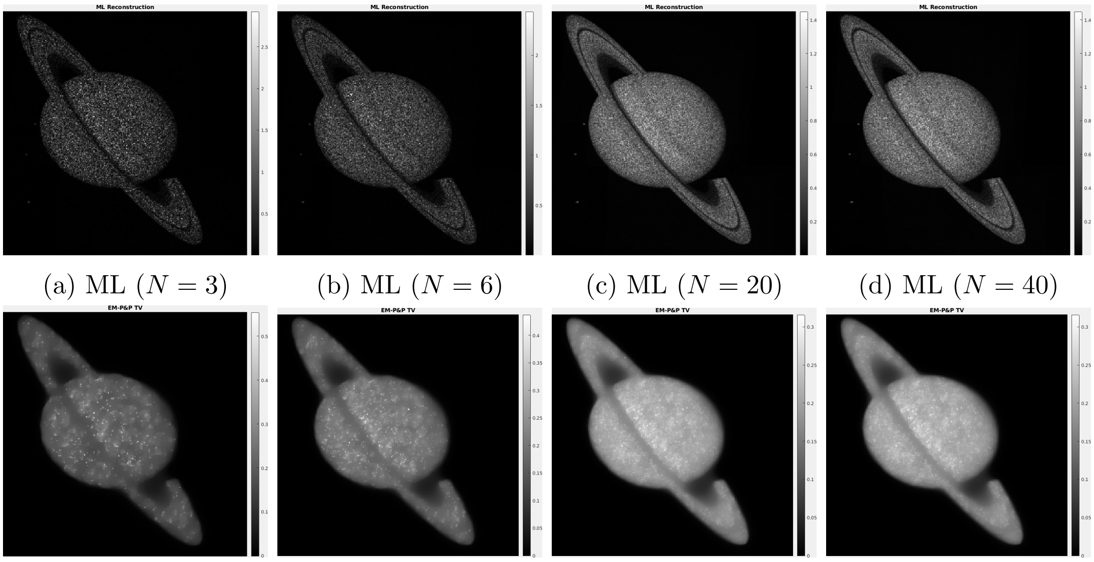

(a) ML ($N = 3$) (b) ML ($N = 6$) (c) ML ($N = 20$) (d) ML ($N = 40$)

(e) PnP-TV ($N = 3$) (f) PnP-TV ($N = 6$) (g) PnP-TV ($N = 20$) (h) PnP-TV ($N = 40$)

Figure 3: Multi-image plug and play algorithm for: For the image with $\sigma_w = 1e^{-3}$.

where $\tilde{r} = v - u$. The operator F is the proximal mapping of $\ell(r)$ and is equivalent to a MAP estimate of r with a Gaussian prior having a distribution $p(r) \sim N(\tilde{r}, \sigma_\lambda^2 I)$.
Specifically when $\ell(r) = -\log p(y|r)$, the inversion operator is given as

$$
\begin{aligned}
F(\tilde{r_i}, \sigma_\lambda) \quad &= \quad \arg\min_{r_i} \left\{ \log(r_i + \sigma_w^2) + \frac{|y_i|^2}{r_i + \sigma_w^2} + \frac{1}{2\sigma_\lambda^2}(r_i - \tilde{r_i})^2 \right\}, \\
&\implies \quad \frac{1}{r_i + \sigma_w^2} - \frac{|y_i|^2}{(r_i + \sigma_w^2)^2} + \frac{1}{\sigma_\lambda^2}(r_i - \tilde{r_i}) = 0, \\
&\implies \quad \sigma_\lambda^2(r_i + \sigma_w^2) - |y_i|^2 + (r_i - \tilde{r_i})(r_i + \sigma_w^2)^2 = 0, \\
&\implies \quad r_i^3 + (-\tilde{r}_i + 2\sigma_w^2)r_i^2 + (-2\tilde{r}_i\sigma_w^2 + \sigma_w^4 + \sigma_\lambda^2)r_i + (\sigma_\lambda^2\sigma_w^2 - \tilde{r}_i\sigma_w^4) = 0.
\end{aligned}
$$

Thus the solution of the inversion-operator is simply the root of the cubic-polynomial. We are constrained that the root of the cubic-polynomial is real.

(2) **Denoising operator**

$$
H(\tilde{v}, \sigma_n) = \arg\min_{v} \left\{ \frac{1}{2\sigma_n^2} \|v - \tilde{v}\|^2 + s(v) \right\}
$$

where $\sigma_n^2 = \beta\sigma_\lambda^2$ and $\tilde{v} = r + u$. The denosing operator H is a proximal mapping of $s(v)$. Mathematically, it is equivalent to a Gaussian denosing operation. Thus, we can replace H with a denoiser which removes noise with a variance σ_n^2. We use the following denoising-operators to use for Gaussian-denosing: (1) TV, (2) BM3D denoiser. The complete PnP algorithm is given in Algorithm 1.

1.3.1 Parameter-tuning

In the following analysis we assume that we know the true-value of σ_w. The parameters to be tuned for the problem are σ_λ, σ_n; which are essentially the tuning parameters for each of the proximal-operators (inversion and denoising).

Algorithm 1 Plug and Play $(y, \sigma_w, \sigma_\lambda, \sigma_n)$

$v = y$, $u = 0$
Repeat
$\{$
$\tilde{r} = v - u$
$r = F(y, \tilde{r}, \sigma_w, \sigma_\lambda)$ **Inversion-Operator**
$\tilde{v} = r + u$
$v = H(\tilde{v}, \sigma_n)$ **Denoising-Operator**
$u = u + (r - v)$
$\}$

1.4 Direct CNN-approach

Recently we have tried another direct CNN approach to directly learn the mapping from $|y|$ to r. In this approach we learn the mapping from $|y|$ to r by training a convolutional neural network (CNN) on the image pairs from the phase-less measurements to the reflectance of the object. The network architecture that we use follows from the network that has been used for the perceptual-loss extraction paper in SRNET [4].
The architecture that we used is outlined in Tables 1. A residual and convolution block is shown in Figures 4. The results of using testing the trained CNN on the test data is shown in Figure 6. An evaluation of the hyperparameter of the learning rate is shown in Figure 5. We note the variation of the training error as the learning-rate parameter is changed in the experiments. The multi-image results with the trained CNN is shown in Figure 10. This figure indicates that it is performing better in comparison to the approach of the plug and play approach used with the EM algorithm.

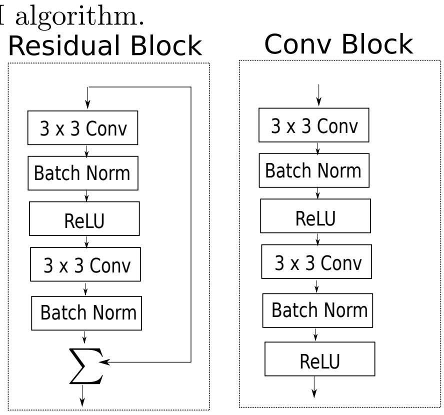

Figure 4: A sample residual and conolutional block.

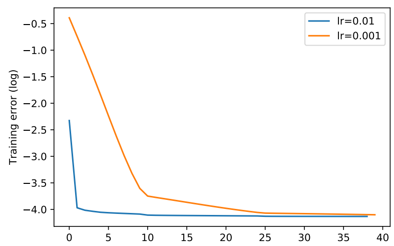

Figure 5: A comparison of training errors for different learning-rates.

Layer	Activation-size
Input	$3 \times 224 \times 224$
$64 \times 9 \times 9$ convBlock	$64 \times 224 \times 224$
Residual block 64 filters	$64 \times 224 \times 224$
Residual block 64 filters	$64 \times 224 \times 224$
Residual block 64 filters	$64 \times 224 \times 224$
Residual block 64 filters	$64 \times 224 \times 224$
$64 \times 3 \times 3$ convBlock	$64 \times 224 \times 224$
$3 \times 9 \times 9$ conv2d	$3 \times 224 \times 224$
batchNormalization	3

Table 1: Network architecture used for the direct CNN based reflectance retrieval.

1.4.1 Perceptual loss-function

Following the paper [4], we investigate the idea of incorporating prior-information from a pre-trained image-classifier into the CNN algorithm that is used for denoising the speckle pattern. Since we are investigating the reconstruction performance of the algorithms on gray-scale images, we trained a gray-scale image classifier. The architecture of the classifier we used is given in the following Figure 8. We use the features from the classifier trained with a different parameter to extract the information from the image. Concretely, we solve the following optimization

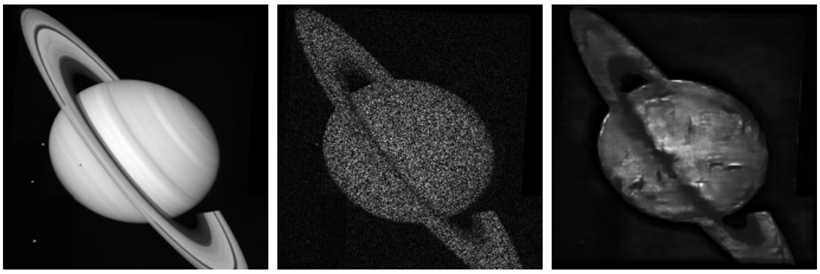

(a) GT (b) Input image (c) Output-Img

Figure 6: The learning-rate used to define this network is 0.01 with a step-decay parameter of 0.1 and a step-list being [10, 25]. The number of training-epochs is 100. We use a deeper-architecture in comparison to the SRNET architecture.

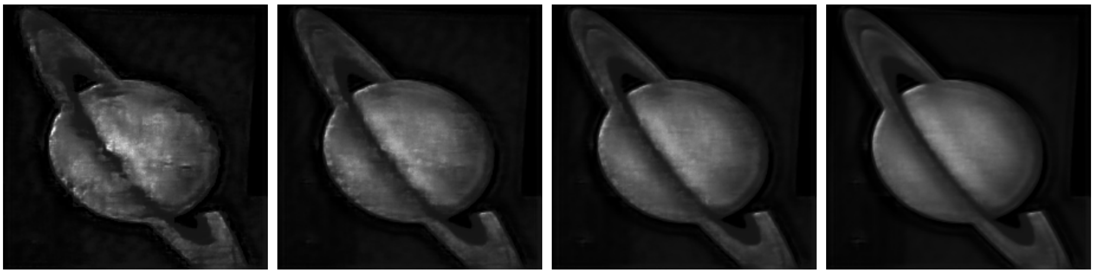

(a) $N = 1$ (b) $N = 3$ (c) $N = 6$ (d) $N = 20$

Figure 7: CNN algorithm applied for multiple images: The noise in each of the images is $\sigma_w = 1e^{-3}$.

problem while we solve for the neural-network:

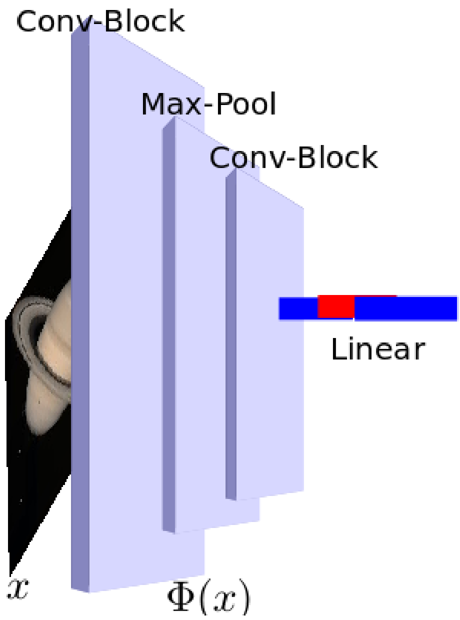

Figure 8: Architecture of the image-classifier

$$NN = \arg\min_{W,b} \|\hat{y} - y\|_2^2.$$

The output from the denoising framework for the different classifiers is given as The results

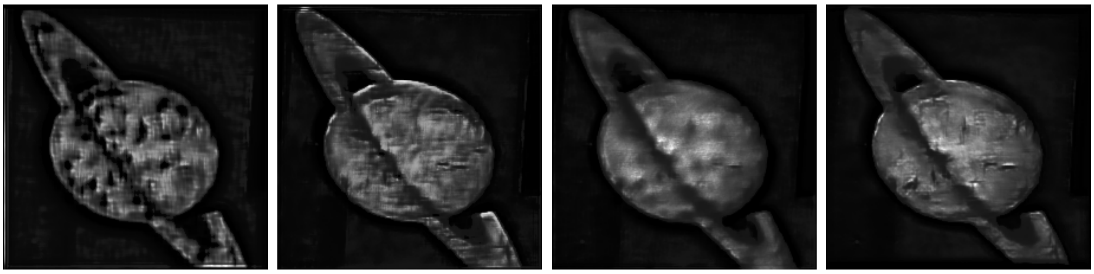

(a) Accuracy: 42% (b) Accuracy: 58% (c) Accuracy: 67% (d) ℓ_2 cost-function

Figure 9: Comparison of perceptual loss and ℓ_2 loss-function.

comparing the performance of the 67% accurate classifier versus the ℓ_2 loss-function for multiple images is given next:

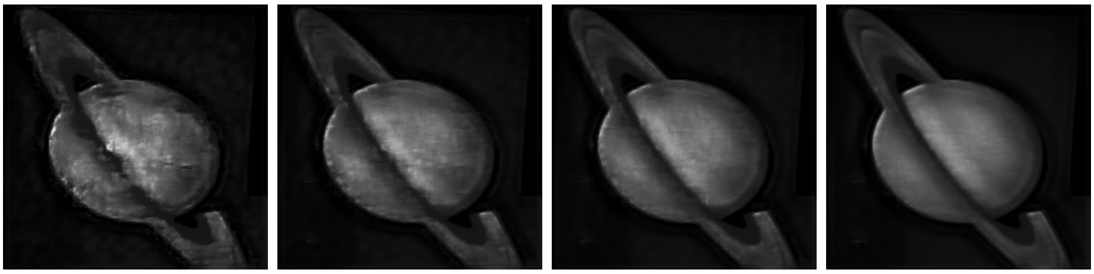

(a) $N = 1$ (b) $N = 3$ (c) $N = 6$ (d) $N = 20$

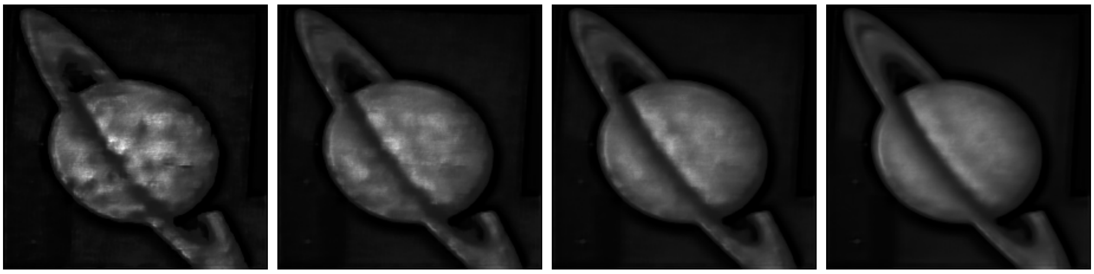

(e) $N = 1$ (f) $N = 3$ (g) $N = 6$ (h) $N = 20$

Figure 10: (a)-(d) Performance of the ℓ_2 loss-classifier. (e)-(h) Performance of the 67% accurate classifier.

1.5 Regularization by denoising

Recently there has been an alternative approach instead of the ADMM or Plug-and-Play (P^3) approach: regularization by denoising [3]. The key idea of the paper is the regularization proposed in the paper:

$$\rho(x) = \frac{1}{2}x^T[x - f(x)],$$

where $f(x)$ is the denosied version of x. The intuition behind this regulaization is:

- Penalty introduced is the inner-product between the candidate image x and its denosing residual.

A small value for $\rho(x)$ implies that

- Residual is very small, image x is at the fixed point or $x \approx f(x)$.
- Cross-correlation between the image x and its residual is very small or alternatively resembles white-noise or contains no image-like features.

1.6 Properties of the denosier $f(x)$

The RED paper assumes that a denoiser can be assumed to be a psuedo-linear filter of the form

$$f(x) = W(x)x.$$

The following properties are further assumed on the denoiser (**to be completed**).

1.7 Solving the regularized optimization problem

A general inverse-problem is of the form

$$\hat{x} = \arg\min_x \quad E(x) \triangleq \ell(x, y) + \frac{\lambda}{2}x^T[x - f(x)].$$

The gradient of the above expression is of the form

$$\begin{aligned} \nabla_x E(x) &= \nabla_x \ell(y, x) + \frac{\lambda}{2}\nabla_x\{x^T(x - f(x))\} \\ &= \nabla_x \ell(y, x) + \lambda(x - f(x)). \end{aligned}$$

With the above formulation, a gradient-descent based iterative approach would consist of the following iterations:

$$\hat{x}_{k+1} = \hat{x}_k - \mu \nabla_x E(x)|_{\hat{x}_k}.$$

1.8 Regularization by denoising for reflectance-estimation

The regularization by denoising approach for the reflectance-reconstruction problem is given as

$$\begin{aligned} \hat{r} &= \arg\min_r \quad \ell(r, y) + \lambda\rho(r) \\ &= \arg\min_r \quad \sum_{i=1}^{N}\left(\log(2\pi(r_i + \sigma_w^2)) + \frac{|y_i|^2}{r_i + \sigma_w^2}\right) + \frac{\lambda}{2}r^T\{r - f(r)\} \\ &= \arg\min_r \quad E(r). \end{aligned}$$

The RED algorithm for using this procedure is of the form

$$\hat{r}_{k+1} = \hat{r}_k - \mu \nabla_r E(r)|_{\hat{r}_k},$$

where

$$\nabla_r E(r_i) \quad = \quad \left(\frac{1}{2\pi(r_i + \sigma_w^2)} - \frac{|y_i|^2}{(r_i + \sigma_w^2)^2} \right) + \lambda(r_i - f(r_i)).$$

Results to be completed...

References

[1] Casey J. Pellizzari et al. *Optically coherent image formation and denoising using a plug and play inversion framework in OSA.*

[2] S. V. Venkatakrishnan et al. *Plug-and-play priors for model based reconstruction in GLOBALSIP.*

[3] Y. Romano et al. *The little engine that could: Regularization by denoising.*

[4] J. Johnson et al. *Perceptual Losses for Real-Time Style Transfer and Super-Resolution.*